Normal transferrin patterns in congenital disorders of glycosylation with Golgi homeostasis disruption: apolipoprotein C-III at the rescue!

Alexandre Raynor, Catherine Vincent-Delorme, Anne-Sophie Alaix, Sophie Cholet, Thierry Dupré, Sandrine Vuillaumier-Barrot, François Fenaille, Claude Besmond, Arnaud Bruneel

Normal transferrin patterns in congenital disorders of glycosylation with Golgi homeostasis disruption: apolipoprotein C-III at the rescue!

Alexandre Raynor[1], Catherine Vincent-Delorme[2], Anne-Sophie Alaix[3], Sophie Cholet[4], Thierry Dupré[1], Sandrine Vuillaumier-Barrot[1], François Fenaille[4], Claude Besmond[5], Arnaud Bruneel[1,6]

Affiliations:

[1] *AP-HP, Biochimie Métabolique et Cellulaire, Hôpital Bichat-Claude Bernard, Paris, France.*

[2] *Service de génétique clinique Guy Fontaine, CHRU de Lille-Hôpital Jeanne de Flandre, Lille, France.*

[3] *Fondation Elan Retrouvé, Université de Paris-Sorbonne Paris Cité, Imagine Institute, INSERM UMR1163, Paris, France*

[4] *Université Paris-Saclay, CEA, INRAE, Département Médicaments et Technologies pour la Santé (DMTS), MetaboHUB, F-91191 Gif sur Yvette, France.*

[5] *Université de Paris-Sorbonne Paris Cité, Imagine Institute, INSERM UMR1163, Paris, France*

[6] *INSERM UMR1193, Mécanismes cellulaires et moléculaires de l'adaptation au stress et cancérogenèse, Université Paris-Sud, Châtenay-Malabry, France.*

Corresponding author: Dr Arnaud Bruneel

Email: arnaud.bruneel@aphp.fr

Address: Hôpital Bichat, Biochimie Métabolique et Cellulaire, 46 rue Henri Huchard, 75018 Paris, France.

Keywords:

apoC-III; ATP6V0A2-CDG; CDG; COG4-CDG; false-negative transferrin; two-dimensional electrophoresis.

Abbreviations

2-DE:	two-dimensional electrophoresis
apoC-III:	apolipoprotein C-III
ACMG:	American college of medical genetics
CDG:	congenital disorder(s) of glycosylation
COG:	conserved oligomeric Golgi
CZE:	capillary zone electrophoresis
IEF:	isoelectric focusing
HC:	head circumference
Hpt:	haptoglobin
MALDI-TOF:	matrix assisted laser desorption/ionization – time of flight
MS:	mass spectrometry
Trf:	transferrin
VUS:	variant of unknown significance

Details of funding: This work was supported by grant ANR-15RAR3-0004-06 under the frame of E-RARE-3, the ERA-Net for Research on Rare Diseases; it was also supported by the European Union's Horizon 2020 research and innovation program under the ERA-NET cofund action N° 643578 (AB, TD, SVB). The "Commissariat à l'Énergie Atomique et aux Énergies Alternatives" and the MetaboHUB infrastructure (ANR-11-INBS-0010 grant) (SC, FF).

Abstract

We identified three cases of congenital disorders of glycosylation (CDG) with Golgi homeostasis disruption, one ATP6V0A2-CDG and two COG4-CDG, with false-negative transferrin screening analyses. Patient 1 (P1) presented at birth with *cutis laxa*. Patient 2 (P2) and patient 3 (P3) are adult siblings and presented with severe symptoms evocative of inborn errors of metabolism.

Targeted gene sequencing in P1 revealed pathogenic *ATP6V0A2* variants, shared by her affected older brother. In P2 and P3, whole exome sequencing revealed a homozygous *COG4* variant of unknown significance. In all affected individuals, transferrin analysis was normal.

Mass-spectrometry based serum N-glycome analysis and two-dimensional electrophoresis (2-DE) of haptoglobin and of mucin core 1 O-glycosylated apolipoprotein C-III (apoC-III) were performed. All results of second-line N-glycosylation analyses were initially normal. However, apoC-III 2-DE revealed characteristic "apoC-III_1" pattern in P1 and specific "apoC-III_0" patterns in P2 and P3. In P2 and P3, this allowed reclassifying the variant as likely pathogenic according to ACMG guidelines.

These cases highlight the existence of normal transferrin patterns in CDG with Golgi homeostasis disruption, putting the clinicians at risk of wrongly misdiagnosing patients. Furthermore, they show the potential of apoC-III 2-DE in diagnosing this type of CDG, with highly specific patterns in COG-CDG.

1. Introduction

Protein glycosylation is a post-translational modification in which a carbohydrate is bound covalently to an amino acid. The two most common types of protein glycosylation are N-glycosylation, where the sugar moiety is bound to an asparagine residue, and O-glycosylation, where it is essentially bound to a threonine or a serine residue [1,2]. Glycosylation results from the action of multiple glycosyltransferases and glycosidases, the activities of which are highly dependent on their biochemical environment (pH, coenzymes, ions…) and on the supply of activated sugars by transporters. Congenital disorders of glycosylation (CDG) constitute a family of over 140 rare inborn errors of metabolism affecting glycosylation pathways, with less than 50 known cases in most of them [3]. Their clinical manifestations are systemic and usually non-specific, and include neurological disorders, hypotonia, hepatopathy, dysmorphia and coagulopathy. Diagnosis is most often difficult and requires careful clinical examination, biochemical and genetic investigations [4].

Historically, biochemical CDG diagnosis was based on serum transferrin (Trf) glycoforms analysis by isoelectric focusing (IEF), which can detect N-glycosylation defects [5]. Two types of Trf patterns were described, leading to a classification of CDG as either type I or type II. In type I CDG (CDG-I), N-glycosylation defects originate from the cytosol or the endoplasmic reticulum and involve various steps of the sugar moiety synthesis and its binding to the protein. In type II CDG (CDG-II), they originate from the Golgi apparatus and involve the protein-bound sugar moiety trimming and maturation. Mutations can affect glycosyltransferases, glycosidases or sugar transporters, or can affect vesicular trafficking, Golgi proton pumps and divalent cation (e.g., manganese Mn^{2+}) transporters: in the latter cases, this leads to Golgi homeostasis disruption, reducing glycosyltransferases activities and/or altering their localization [6-8]. In CDG-II with Golgi homeostasis disruption, both N-glycosylation and mucin core 1 O-glycosylation are generally affected.

Since the initial description of CDG, additional biochemical analyses have been developed, notably including study of serum N-glycome by mass spectrometry (MS) [9] and study of mucin core 1 O-glycosylation by electrophoretic or MS analysis of apolipoprotein C-III (apoC-III) [10-12]. Both techniques may highlight characteristic profiles suggestive of particular CDG, helping with diagnosis. N-glycome is of use in all CDG-II, whereas apoC-III is of use in CDG-II with Golgi homeostasis disruption [12]. Although classically used as second-line laboratory tools, these techniques may also help in screening cases with mild Trf glycosylation abnormalities or cases in which Trf analysis may have limited value (e.g., first weeks of life, Trf protein variants) [13,14].

In this work, we describe three new cases of CDG with Golgi homeostasis disruption (one ATP6V0A2-CDG and two COG4-CDG affected individuals) where Trf patterns were normal, putting the clinicians at risk of wrongly discarding CDG diagnoses. We first describe the clinical presentation of each affected individual and the genetic tests that were performed. We then describe the second-line biochemical investigations that were conducted, and how successful diagnoses were made thanks to apoC-III two-dimensional electrophoresis.

2. Materials and methods

2.1 Transferrin capillary zone electrophoresis

Trf capillary zone electrophoresis (CZE) was performed on the Capillarys 2 Flex Piercing (Sebia, France), using the Capillarys CDT kit, as previously described [15]. Briefly, after iron treatment, Trf glycoforms are separated whilst migrating through a silica capillary and detected at 200 nm. Signals are processed by the Sebia Phoresis software for interpretation.

2.2 Two-dimensional electrophoresis of haptoglobin and apolipoprotein C-III

Two-dimensional electrophoresis (2-DE) of serum haptoglobin (Hpt; a N-glycosylated protein) and apoC-III was conducted as previously described [10,16]. Briefly, IEF was performed on a ZOOM Strip (pH 4-7) and SDS-PAGE was performed on a NuPAGE Bis-Tris gel (4-12%) (Thermo Fisher Scientific). Proteins were transferred onto nitrocellulose and the membrane was incubated in TTBS - 5% milk with the rabbit primary antibody (respectively, anti-Hpt, 1/3000 v/v; Dako and anti-apoC-III, 1/5000 v/v; BioDesign international) and then with the secondary antibody (1/5000 v/v, GE Healthcare). Revelation was performed using Clarity ECL reagent and profiles were acquired with an XRS Chemidoc camera (Bio-Rad).

2.3 Total serum N-glycome analysis by matrix-assisted laser desorption/ionization time-of-flight mass spectrometry (MALDI-TOF MS).

Analysis of serum N-glycans by MALDI-TOF MS was performed as described before [17,18]. Briefly, serum samples (5 µL) were diluted in 100 mM sodium phosphate buffer (pH 7.4) and 100 mM dithiothreitol solutions (final concentrations 20 mM and 10 mM, respectively) and denatured by heating at 95°C for 5min for protein denaturation. Protein de-N-glycosylation was accomplished with 2 U of peptide-N-glycosidase F (PNGase F) following an overnight incubation at 37°C. After acidification, proteins were precipitated using ice-cold ethanol for 1 h at -20°C. Released N-glycans were purified using porous graphitic carbon solid phase extraction cartridges (Thermo Fisher Scientific), and subsequently permethylated before another purification step using C18 spin-columns (Thermo Fisher Scientific). After drying, the purified permethylated N-glycans were resuspended in 10 µL of a 50% methanol solution. N-glycan samples (0.5 µL) were spotted on the MALDI target plate and thoroughly mixed with 0.5 µL of a 2,5-dihydroxybenzoic acid solution (10 mg/mL in 50% methanol containing 10 mM sodium acetate). The analysis was performed on an UltrafleXtreme mass spectrometer operated

in the reflectron positive ion mode (Bruker Daltonics) using a 2 kHz laser repetition rate. A 20 kV acceleration voltage and an extraction delay of 130 ns were used. The spectra were obtained by accumulating about 5000 shots within an m/z range of 1000–5000. The MALDI-TOF mass spectra were internally calibrated, and further processed using the GlycoWorkBench software [19].

2.4 Genetic studies

For P1, targeted gene sequencing using fluorescent detection (Big Dye terminator v1.1, Sanger sequencing) was performed after informed consent on ABI 3130 (Applied Biosystem), to search for the pathogenic variants previously found in her brother in intron 5 and exon 18 of *ATP6V0A2* gene.

For P2, P3, whole exome sequencing of patients and their parents was performed after informed consent and approval by the Institution Review Board of Ile de France (Approval ≠ 2015- 03-03/DC 2014–2272, Paris, France). Libraries were prepared from circulating white cells, using an optimised SureSelect Human Exome kit (Agilent). Captured, purified and clonally amplified libraries targeting exonic sequences were sequenced on a HiSeq 2500 (Illumina). Sequence reads were aligned to the human genome (hg19) using BWA software. Downstream processing was carried out with the Genome analysis (GATK), SAM and Picard Toolkits.

Single nucleotide variants and indels were subsequently called by the SAMtools suite (mpileup, bcftools, vcfutil). All calls with a read coverage ≤5× and a Phred-scaled single nucleotide polymorphism (SNP) quality ≤20 were filtered out. Substitution and variation calls were made with the SAMtools pipeline (mpileup). Variants were annotated with an in-house Paris Descartes University bioinformatics platform pipeline based on the Ensembl database (release 67). *De novo*, recessive and X-linked inheritance was applied for candidate gene identification. After exome analysis, each selected variant was confirmed by direct sequencing using

BigDyedideoxy terminator chemistry on an ABI3130xl genetic DNA analyzer (Applied Biosystems) after PCR.

3. Results

3.1 Clinical presentations

At birth, P1 (**Figure 1**) had normal weight, height, and head circumference (HC) and presented dystonia, facial dysmorphia, plagiocephaly and *cutis laxa*. At 2.5 months old, she experienced developmental delay, with her weight and height at -1 SD and HC at -2.5 SD. *Cutis laxa* was persistent, with single transverse palmar creases. She was able to smile. At 5.5 months old, she had *cutis laxa*, joint hyperlaxity and an enlarged anterior fontanel. At 7 months old, she still experienced developmental delay with -2 SD height, weight at -1 SD and HC at -3.5 SD. She had pallor of skin and conjunctiva associated with a discrete anemia (hemoglobin at 11 g/dL) and her *cutis laxa* deteriorated. Her tonus was satisfying. She had atypical upper limb movements (potentially dysmetria). At 2 years old, she started walking and presented *cutis laxa*, facial dysmorphia, microcephaly (-3 SD) and language delay. In the first two years of her life, she experienced multiple episodes of severe bronchiolitis, requiring hospitalization, and asthma requiring treatment. Biochemically, recurrent episodes of hypocalcemia were noted.

P2 and P3 were born to healthy, first cousin Tunisian parents of Jewish ancestry after normal pregnancy and term delivery. P2, a male, had developmental delay, spasticity and global dystonia. He had growth retardation (weight, height and HC all below -4 SD). He also had orofacial dyspraxia with hypotonic face and open mouth. P3, a girl, had a similar clinical course as her brother. At the age of 6 months, she had delayed psychomotor skills, global dystonia (reportedly more severe than P2), spasticity and nystagmus. Her face was hypotonic with orofacial dyspraxia. She had microcephaly (-3 SD), and growth retardation (-3 SD for weight

and height). Mild dysmorphic features included hypertelorism and epicanthus. At 19 and 22 years, the two siblings are wheelchair-bound, with global developmental delay, absent speech, good non-verbal interaction and correct understanding of short sentences. Clinical examination showed tetra pyramidal spasticity, dystonia, orofacial dyspraxia and microcephaly (-4 SD). Metabolic work up including peroxisomal and lysosomal investigations was unremarkable and brain CT scan and MRI were normal.

3.2 Genetics

In P1, targeted gene sequencing revealed compound ATP6V0A2 heterozygosity. The first variant was a c.522-3_522-2del intronic deletion in intron 5, inherited from her father. This 2bp deletion was not described in literature nor listed in gnomAD or dbSNP databases. This variant alters the splice acceptor site of exon 6. While it was not possible to predict protein alterations induced by this variant, skipping of exon 6 seemed probable. Second variant was a c.2293C>T; p.Gln765* exonic nonsense variant on exon 18, inherited from her mother and known in gnomAD at a 0.0025% frequency, in dbSNP (rs80356758) and already described as pathogenic variant in ClinVar.

In P2 and P3, a missense variant in COG4 (c.15G>A; p.Met5Ile, NM_015386.2) was found at the homozygous state. The variant has been previously reported in GnomAD at a 0.00041% frequency and in dbSNP (rs1265929563). The variant was predicted pathogenic by Mutation Taster (http://www.mutationtaster.org) but tolerated by Sift (http://sift.jvci.org) and Polyphen2 (http://genetics.bwh.harvard.edu/pph2). The methionine in position 5 corresponds to the Met1 start codon in some species. Their parents and healthy brother were heterozygote carriers. The healthy sister was homozygous for the wild-type allele. According to ACMG guidelines, this variant was initially classified as variant of unknown significance (VUS). However, a functional

assay supported the deleterious nature of this *COG4* variant (apoC-III analysis, see below), thus subsequently reclassifying it as a likely pathogenic variant.

3.3 Transferrin capillary zone electrophoresis (CZE) patterns

Trf CZE electrophoregrams are presented in **Supplemental Figure 1** and the proportions of its glycoforms are indicated in **Table 1**. In healthy subjects, Trf is mostly 4-sialylated (reference range: 78-86 %), with 5-sialo, 3-sialo (< 6 %) and 2-sialo (< 1.6 %) glycoforms also being present in lower proportions. Regarding P1, Trf profiles were normal at 1 and 3 months old. At 8 months old, Trf profile was abnormal, with diminished 4-sialo-Trf (75.3%) and elevated 3-sialo-Trf (13.4 %), compatible with CDG-II. Regarding P2 and P3, Trf profiles were normal at all ages. For information, P1's brother's Trf glycoforms are also indicated in **Table 1**. With diminished 4-sialo-Trf, elevated 3-sialo-Trf (24.2 %), 2-sialo-Trf (2.7 %), and the abnormal presence of 1-sialo-Trf (0.1 %), his profile was clearly abnormal and evocative of CDG-II.

3.4 Two-dimensional electrophoresis of serum haptoglobin

Serum Hpt 2-DE patterns are presented in **Supplemental Figure 2**. Compared to a healthy subject (a), Hpt profiles of P1 were normal at 1 and 3 months old (b, c). At 8 months old (d), an additional faint spot migrating cathodically can be noted (arrow) in agreement with a CDG-II pattern. Regarding P2, Hpt profiles (e, f) were normal at all ages. For P3 (g), a faint abnormal cathodical spot can be observed (arrow).

3.5 Profiling of total serum N-glycans by MALDI-TOF mass spectrometry

Total serum N-glycans were analyzed by MALDI-TOF MS for the 3 patient samples withdrawn at different time points. Corresponding profiles are presented in **Supplemental Figure 3** and

proved similar to what can be commonly observed for a healthy subject. Therefore, those profiles were not clearly evocative of any CDG-II occurrence.

3.6 Two-dimensional electrophoresis of serum apoC-III

ApoC-III 2-DE patterns are presented in **Figure 2** and the proportions of its glycoforms are indicated in **Table 2**. In healthy subjects, apoC-III_2 (disialylated), apoC-III_1 (monosialylated) and apoC-III_0 (non-glycosylated) represent 25 - 60 %, 40 - 75 % and < 5 % of total apoC-III, respectively [10]. Regarding P1, at 1 month old, apoC-III profile was abnormal, with increased apoC-III_1 (87 %) and decreased apoC-III_2 (13 %), and with no detectable non-glycosylated apoC-III_0. This corresponded to an "apoC-III_1" profile. Similar profiles were found at 3 months old, with apoC-III_2 and apoC-III_1 representing 7 % and 93 % of total apoC-III, respectively, and at 8 months old, where they represented 12 % and 88 %, respectively. For P2 at 21 years old, apoC-III profile was abnormal, with increased apoC-III_1 (82 %), increased non-glycosylated apoC-III_0 (6 %), and decreased apoC-III_2 (12 %). This corresponded to an "apoC-III_0" 2-DE profile. At 22 years old, apoC-III_2 remained decreased (21 %), apoC-III_1 was in normal proportion and non-glycosylated apoC-III_0 was at the threshold value (5 %). Regarding P3, apoC-III profile was clearly abnormal, with markedly increased non-glycosylated apoC-III_0 (10 %), and with apoC-III_2 and apoC-III_1 in normal proportions, corresponding to a typical COG-CDG "apoC-III_0" 2-DE profile.

4. Discussion

Since the first description of PMM2-CDG by Jaeken *et al*. in 1984 [5], the advances in clinical biochemistry and genetics have led to a rapid expansion of the CDG family. More recently, a CDG subfamily characterized by Golgi homeostasis disruption and a type II Trf pattern has been identified, where mutations are found on genes coding for Golgi proton pump subunits

[7], vesicular traffic proteins [6] and Mn^{2+} transporters [8], resulting in decreased glycosyltransferases catalytic activities and/or altered localization. Conserved Oligomeric Golgi (COG) complex subunits (COG1 to COG8) are Golgi proteins involved in retrograde vesicular transport. Defective COG proteins/complex lead to improper addressing and recycling of glycosyltransferases. Since N-glycan chain maturation and O-glycan chain synthesis depend on the sequential and ordered action of glycosyltransferases, COG-CDG thus cause defects in N- and mucin type O-glycosylation. In 2004, Wu *et al*. [20] described the first CDG belonging to this subfamily, COG7-CDG. Since the description of COG7-CDG, new COG-CDG have been described affecting every COG protein except COG3 [6]. COG-CDG are now believed to be rather frequent among CDG-II [21]. In 2008, Kornak *et al.* [7] described the first CDG with Golgi pH disruption, ATP6V0A2-CDG. This CDG is characterized by mutations affecting the α_2 subunit of the V0 domain of the Golgi V-ATPase. V-ATPase imports protons into the Golgi apparatus and thus creates a pH gradient between cis- and trans-Golgi, with trans-Golgi being more acidic. A defective V-ATPase leads to disruption of this acidic gradient [22]. Since glycosyltransferases are pH-dependent, ATP6V0A2-CDG thus causes defects in N- and mucin type O-glycosylation. Since the description of ATP6V0A2-CDG, new CDG-II with Golgi pH disruption have been described affecting other V-ATPase subunits or V-ATPase associated proteins [23]. More recently, CDG with defective Golgi Mn^{2+} transporters have also been described, including TMEM165-CDG [24] and SLC39A8-CDG [25], also with combined N- and O-glycosylation defects.

In 2003, Wopereis *et al.* [11] designed an IEF technique to study mucin core 1 O-glycosylation of apoC-III and discovered characteristic patterns in patients with primary and secondary defects in N-glycosylation. Thereafter, "apoC-III_0" IEF patterns with abnormally elevated asialylated apoC-III_0 and "apoC-III_1" IEF patterns with abnormally elevated monosialylated apoC-III_1 were notably linked to COG-CDG and to ATP6V0A2-CDG, respectively. Bruneel *et*

al. [10] refined this technique by adding a second dimension (2-DE), allowing to separate all asialylated forms of apoC-III by molecular weight. This offers additional information over IEF alone, which is of help in defining particular CDG patterns. Notably, 2-DE can differentiate between the non-glycosylated and mucin core 2 asialylated apoC-III glycoforms [26] with, in our 10-year experience (over one thousand apoC-III patterns performed in our laboratory), a 100 % specificity of the non-glycosylated apoC-III_0 2-DE patterns towards diagnosed COG-CDG cases (n = 8) [12].

In this work, we describe three new cases of CDG with Golgi homeostasis disruption and who had normal Trf analyses results: one ATP6V0A2-CDG and two COG4-CDG affected individuals.

At 2 months old, P1 presented *cutis laxa*, a characteristic symptom of ATP6V0A2-CDG, and her brother was known to be affected by this disease (unpublished case). Therefore, targeted gene sequencing was requested, and results were in favour of ATP6V0A2-CDG, with the same pathogenic variant as her brother. However, by stark contrast with her brother, P1's Trf CZE profile was normal at 2 months. Since her clinical presentation and her *ATP6V0A2* variants were in favour of the disease, additional investigations were conducted. Firstly, 2-DE of serum haptoglobin was realized. We previously showed [16] that this technique could detect N-glycosylation defects when Trf analysis was inconclusive (e.g., Trf protein variants, liver failure…). Regarding P1, results were also normal, initially at 2 months. Secondly, total serum N-glycome was studied by MALDI-TOF MS. Such an approach allows detection and characterization of N-glycosylation defects in a wide range of glycoproteins simultaneously, which can be applied to CDG diagnosis [4,27]. In CDG with Golgi homeostasis disruption, whilst no characteristic N-glycome patterns have been described, a variety of defects can be evidenced, pointing at a global alteration of N-glycan chains maturation [27]. Regarding P1, results were normal. Thus, neither Hpt analysis nor MALDI-TOF MS supplied any additional

information compared to Trf analysis, at least initially. Following unsuccessful studies of N-glycosylation, study of mucin core 1 O-glycosylation was performed using 2-DE of apoC-III. Regarding P1, an "apoC-III_1" pattern, characteristic of ATP6V0A2-CDG, was found at 2 months old. This result, along with clinical presentation and genetics, allowed to suggest a probable ATP6V0A2-CDG diagnosis even though Trf analysis was normal initially and neither Hpt study nor MS displayed any evidence of disease. ApoC-III analysis therefore appeared more sensitive than the other analyses. At 8 months old, Trf CZE came back positive, an "apoC-III_1" pattern was retrieved, while N-glycome remained normal. This offered reassurance regarding the diagnosis and showed that Trf CZE might be more sensitive than serum N-glycome for highlighting slight N-glycan modifications.

P2 and P3 were seen at 21 and 25 years old, respectively. Their parents were related. Clinically, both patients showed severe signs evocative of inborn errors of metabolism, with global development delay, neurological disorders and microcephaly. Exome sequencing highlighted a homozygous *COG4* missense variant in both affected individuals, suspected to be pathogenic by some prediction software. Their siblings were healthy, with one being homozygous for the wild-type allele, and one being heterozygous for the identified mutation. Both parents were heterozygous for this mutation. In both affected individuals, Trf profiles were normal. Additional studies were performed to document the deleterious nature of this variant, as described for P1. Regarding N-glycosylation, all results were normal in both patients, apart from a slightly abnormal Hpt 2-DE profile in P3. Furthermore, 2-DE of apoC-III revealed a marked "apoC-III_0" 2-DE pattern in P3, and a more discrete "apoC-III_0" 2-DE pattern in P2. In the current state of our knowledge, no false-positive "apoC-III_0" profile has been found in 2-DE. These results, along with similar clinical phenotype and identical *COG4* genotypes, were strongly evocative of a COG4-CDG diagnosis in both affected siblings. As with P1, Trf analyses were normal and only 2-DE of apoC-III allowed establishing a diagnosis. Moreover,

these functional results, according to ACMG's guidelines, converted the p.Met5Ile COG-4 variant from a VUS into a likely pathogenic variant.

These three cases highlight (i) the major role of biochemical analyses in CDG diagnosis, (ii) the occurrence of normal Trf patterns, here in CDG with Golgi homeostasis disruption and (iii), how 2-DE of apoC-III can help establish the right diagnosis. Clinicians who may be consulted by potential CDG-affected individuals must be aware of the occurrence of normal Trf results that put them at risk of misdiagnosing. These three cases may also illustrate a known phenomenon, in which children in the first weeks or life or adult individuals may have falsely negative Trf screening. This has been notably described in PMM2-CDG and may be linked to age-related differences and/or adjustments in protein N-glycosylation [13,28].

In CDG with Golgi homeostasis disruption, 2-DE of apoC-III appears of particular interest as it seems to be more sensitive than N-glycosylation analyses for evidencing such CDG. Of note, the apparent lack of sensitivity of global serum N-glycome analysis for these affected individuals could be linked to subtle and possibly tissue-dependent impacts of these CDG on N-glycosylation, with most circulating N-glycoproteins being unaffected.

2-DE of apoC-III offers further advantages: it is relatively quick to perform and does not necessitate expensive equipment. In some CDG, it can display characteristic patterns, which may be of help in establishing diagnosis, as evidenced in this work with ATP6V0A2-CDG and COG4-CDG. However, it also has flaws: even though it is very sensitive, it is also overall less CDG-specific than Trf analysis, and acquired "apoC-III_1" or "apoC-III_2" patterns have been described in obese patients and in patients with hepatopathies, respectively [29]. 2-DE of apoC-III is a manual assay that must be performed by a specially trained technologist. These flaws led our laboratory to abandon 2-DE of apoC-III as a first intention analysis in patients with potential CDG, only to be used in second line after detection of a CDG-II Trf pattern. However, we show that when clinical presentations and genetics are highly suggestive of CDG with Golgi

homeostasis disruption, 2-DE of apoC-III may be of great help as a first intention analysis or after a normal Trf analysis.

5. Conclusion

In this work, we described three cases of Trf false-negative screening results in CDG affected individuals with Golgi homeostasis disruption, and we showed how 2-DE of apoC-III, a high-resolution technique to study mucin core 1 O-glycosylation, helped establish the right diagnoses. In the absence of a "one-size-fits-all" CDG biomarker, clinical biochemists should pursue the discovery and development of novel biomarkers in order to ensure optimal and timely diagnosis of all CDG affected individuals.

6. Tables

Table 1. Proportions of Trf glycoforms separated by CZE, in %. In bold, abnormal % values. y.o: years old; m.o: months old.

Trf glycoforms	4-sialo	3-sialo	2-sialo	1-sialo	0-sialo
Normal % values	78-86	< 6	< 1.6	0	0
P1 (1; 3; 8 m.o)	88.7 80.1 **75.3**	2.1 5.6 **13.4**	0.3 0.3 0	0 0 0	0 0 0
P1 brother (1 y.o)	**63.4**	**24.2**	**3.7**	**0.1**	0
P2 (19; 21; 22 y.o)	84.0 83.9 83.8	2.9 3.1 2.9	0.7 0.6 0.7	0 0 0	0 0 0
P3 (25 y.o)	83.9	5.0	0.6	0	0

Table 2. Proportions of apoC-III glycoforms, separated by 2-DE, in %. In bold, abnormal % values.

apoC-III glycoforms	apoC-III_2	apoC-III_1	apoC-III_0
Normal % values	25-60	40-75	< 5
P1 (1; 3; 8 m.o)	**13** **7** **12**	**87** **93** **88**	0 0 0
P2 (21; 22 y.o)	**12** **21**	**82** 75	**6** **5**
P3 (25 y.o)	26	64	**10**

7. Figures captions

Figure 1. Photographs of P1. In (A), notice the peculiar morphology, with drooping full cheeks, eversion of the lower eyelids, elongated philtrum, marked Cupid's bow, gaping mouth, large and prominent cupped ears and strabismus. In (B), *cutis laxa*, in particular in the periumbilical region.

Figure 2. apoC-III two-dimensional electrophoresis patterns of the three patients. Negative and positive (COG7-CDG) patterns are shown on top. Proteins are separated according to molecular weight (Mw) and charge. For P1, clear "apoC-III_1" patterns with pathologically increased apoC-III_1 are noticeable at 1 (P1-1), 3 (P1-2) and 8 (P1-3) months old. For P2, a characteristic "apoC-III_0" pattern, with pathologically increased apoC-III_0 is noticeable at 21 (P2-1) but not at 22 (P2-2) years old. For P3, an "apoC-III_0" pattern is evident at 25 years old.

8. References

[1] Stanley P, Taniguchi N, Aebi M. N-Glycans. In: Varki A, Cummings RD, Esko JD, Stanley P, Hart GW, Aebi M, et al., editors. Essentials of Glycobiology [Internet]. 3rd ed. Cold Spring Harbor (NY): Cold Spring Harbor Laboratory Press; 2015. http://www.ncbi.nlm.nih.gov/books/NBK453020/

[2] Wopereis S, Lefeber DJ, Morava É, Wevers RA. Mechanisms in Protein O-Glycan Biosynthesis and Clinical and Molecular Aspects of Protein O-Glycan Biosynthesis Defects: A Review. Clin Chem. 2006;52(4):574-600.

[3] Ondruskova N, Cechova A, Hansikova H, Honzik T, Jaeken J. Congenital disorders of glycosylation: Still "hot" in 2020. Biochim Biophys Acta BBA - Gen Subj. 2021;1865(1):129751.

[4] Bruneel A, Cholet S, Tran NT, Mai TD, Fenaille F. CDG biochemical screening: Where do we stand? Biochim Biophys Acta Gen Subj. 2020;1864(10):129652.

[5] Jaeken J, van Eijk HG, van der Heul C, Corbeel L, Eeckels R, Eggermont E. Sialic acid-deficient serum and cerebrospinal fluid transferrin in a newly recognized genetic syndrome. Clin Chim Acta. 1984;144(2-3):245-7.

[6] D'Souza Z, Taher FS, Lupashin VV. Golgi inCOGnito: From vesicle tethering to human disease. Biochim Biophys Acta Gen Subj. 2020;1864(11):129694.

[7] Kornak U, Reynders E, Dimopoulou A, van Reeuwijk J, Fischer B, Rajab A, et al. Impaired glycosylation and cutis laxa caused by mutations in the vesicular H+-ATPase subunit ATP6V0A2. Nat Genet. 2008;40(1):32-4

[8] Foulquier F, Legrand D. Biometals and glycosylation in humans: Congenital disorders of glycosylation shed lights into the crucial role of Golgi manganese homeostasis. Biochim Biophys Acta Gen Subj. 2020;1864(10):129674.

[9] Guillard M, Morava E, van Delft FL, Hague R, Körner C, Adamowicz M, et al. Plasma N-glycan profiling by mass spectrometry for congenital disorders of glycosylation type II. Clin Chem. 2011;57(4):593-602.

[10] Bruneel A, Robert T, Lefeber DJ, Benard G, Loncle E, Djedour A, et al. Two-dimensional gel electrophoresis of apolipoprotein C-III and other serum glycoproteins for the combined screening of human congenital disorders of O- and N-glycosylation. Proteomics Clin Appl. 2007, 1(3):321-4. 10.

[11] Wopereis S, Grünewald S, Morava É, Penzien JM, Briones P, García-Silva MT, et al. Apolipoprotein C-III Isofocusing in the Diagnosis of Genetic Defects in O-Glycan Biosynthesis. Clin Chem. 2003;49(11):1839-45.

[12] Yen-Nicolaÿ S, Boursier C, Rio M, Lefeber DJ, Pilon A, Seta N, et al. MALDI-TOF MS applied to apoC-III glycoforms of patients with congenital disorders affecting O-glycosylation. Comparison with two-dimensional electrophoresis. Proteomics Clin Appl.

2015;9(7-8):787-93.

[13] Thiel C, Meßner-Schmitt D, Hoffmann GF, Körner C. Screening for congenital disorders of glycosylation in the first weeks of life. J Inherit Metab Dis. 2013;36(5):887-92.

[14] Guillard M, Wada Y, Hansikova H, Yuasa I, Vesela K, Ondruskova N, et al. Transferrin mutations at the glycosylation site complicate diagnosis of congenital disorders of glycosylation type I. J Inherit Metab Dis. 2011;34(4):901-6.

[15] Parente F, Ah Mew N, Jaeken J, Gilfix BM. A new capillary zone electrophoresis method for the screening of congenital disorders of glycosylation (CDG). Clin Chim Acta. 2010;411(1-2):64-6.

[16] Bruneel A, Habarou F, Stojkovic T, Plouviez G, Bougas L, Guillemet F, et al. Two-dimensional electrophoresis highlights haptoglobin beta chain as an additional biomarker of congenital disorders of glycosylation. Clin Chim Acta. 2017; 470:70-4.

[17] Goyallon A, Cholet S, Chapelle M, Junot C, Fenaille F. Evaluation of a combined glycomics and glycoproteomics approach for studying the major glycoproteins present in biofluids: Application to cerebrospinal fluid. Rapid Commun Mass Spectrom. 2015;29(6):461-73.

[18] Bruneel A, Cholet S, Drouin-Garraud V, Jacquemont ML, Cano A, Mégarbané A, et al. Complementarity of electrophoretic, mass spectrometric, and gene sequencing techniques for the diagnosis and characterization of congenital disorders of glycosylation. Electrophoresis. 2018; 39(24):3123-3132.

[19] Ceroni A, Maass K, Geyer H, Geyer R, Dell A, Haslam SM. GlycoWorkbench: a tool for the computer-assisted annotation of mass spectra of glycans. J Proteome Res. 2008;7(4):1650-9.

[20] Wu X, Steet RA, Bohorov O, Bakker J, Newell J, Krieger M, et al. Mutation of the COG complex subunit gene COG7 causes a lethal congenital disorder. Nat Med. 2004;10(5):518-23.

[21] Reynders E, Foulquier F, Leão Teles E, Quelhas D, Morelle W, Rabouille C, et al. Golgi function and dysfunction in the first COG4-deficient CDG type II patient. Hum Mol Genet. 2009;18(17):3244-56.

[22] Eaton AF, Merkulova M, Brown D. The H^+-ATPase (V-ATPase): from proton pump to signaling complex in health and disease. Am J Physiol-Cell Physiol. 2021;320(3):C392-414.

[23 Jansen JC, Cirak S, van Scherpenzeel M, Timal S, Reunert J, Rust S, et al. CCDC115 Deficiency Causes a Disorder of Golgi Homeostasis with Abnormal Protein Glycosylation. Am J Hum Genet. 2016;98(2):310-21.

[24] Foulquier F, Amyere M, Jaeken J, Zeevaert R, Schollen E, Race V, et al. TMEM165 deficiency causes a congenital disorder of glycosylation. Am J Hum Genet. 2012;91(1):15-26.

[25] Park JH, Hogrebe M, Grüneberg M, DuChesne I, von der Heiden AL, Reunert J, et al. SLC39A8 Deficiency: A Disorder of Manganese Transport and Glycosylation. Am J Hum

Genet. 2015;97(6):894-903.

[26] Nicolardi S, van der Burgt YEM, Dragan I, Hensbergen PJ, Deelder AM. Identification of new apolipoprotein-CIII glycoforms with ultrahigh resolution MALDI-FTICR mass spectrometry of human sera. J Proteome Res. 2013;12(5):2260-8.

[27] Bakar NA, Lefeber DJ, Scherpenzeel M van. Clinical glycomics for the diagnosis of congenital disorders of glycosylation. J Inherit Metab Dis. 2018;41(3):499-513.

[28] Hahn SH, Minnich SJ, O'Brien JF. Stabilization of hypoglycosylation in a patient with congenital disorder of glycosylation type Ia. J Inherit Metab Dis. 2006;29(1):235-7.

[29] Harvey SB, Zhang Y, Wilson-Grady J, Monkkonen T, Nelsestuen GL, Kasthuri RS, et al. O-glycoside biomarker of apolipoprotein C3: responsiveness to obesity, bariatric surgery, and therapy with metformin, to chronic or severe liver disease and to mortality in severe sepsis and graft vs host disease. J Proteome Res. 2009;8(2):603-12.

Figure 1

A)

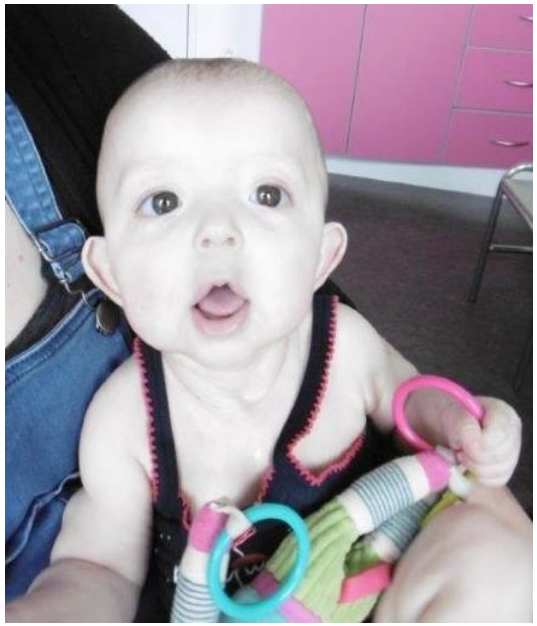

B)

Figure 2

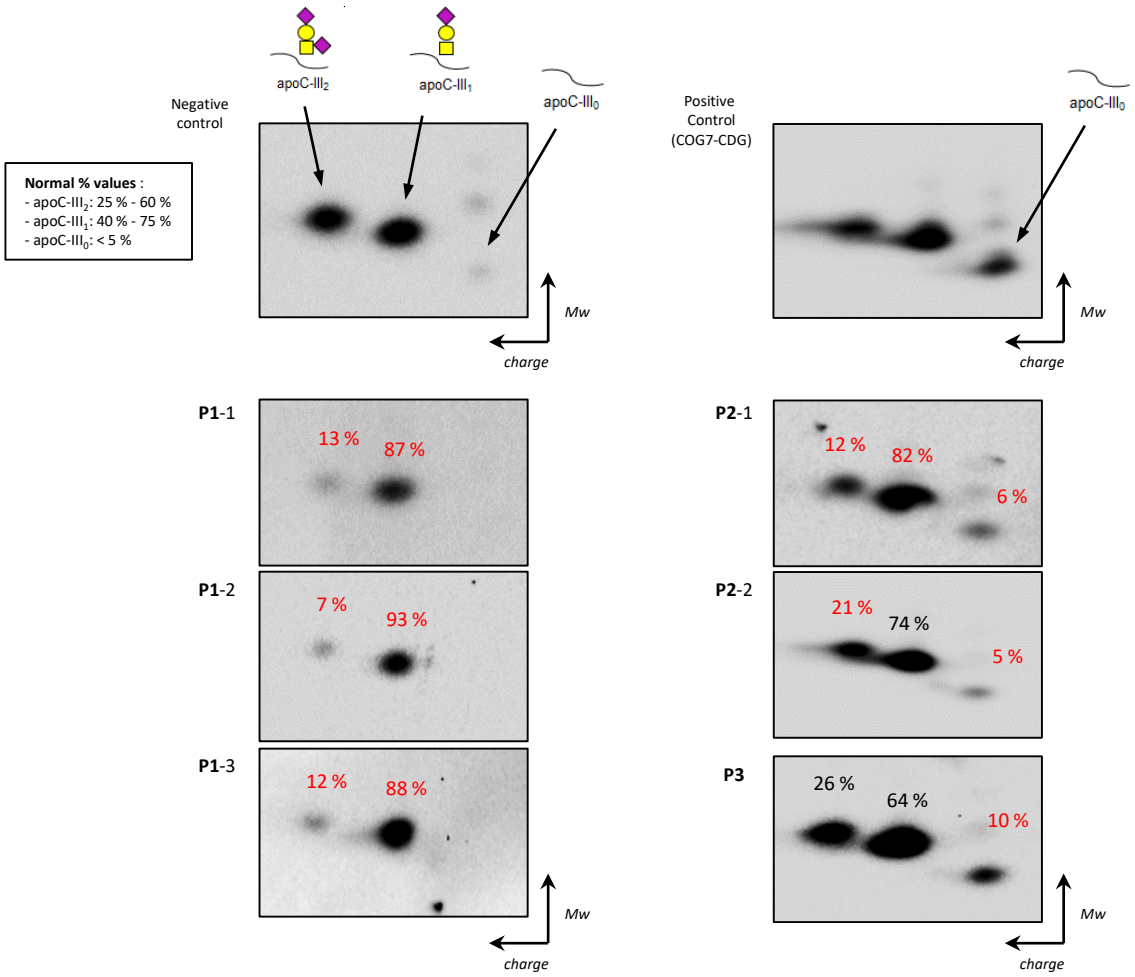
Normal % values :
- apoC-III2: 25 % - 60 %
- apoC-III1: 40 % - 75 %
- apoC-III0: < 5 %
Negative control
apoC-III2
apoC-III1
apoC-III0
Mw
charge
P1-1
13 %
87 %
P1-2
7 %
93 %
P1-3
12 %
88 %
Positive Control (COG7-CDG)
P2-1
12 %
82 %
6 %
P2-2
21 %
74 %
5 %
P3
26 %
64 %
10 %